Journal of Engineering Physics and Thermophysics, Vol. 72, No. 3, 1999

DETERMINATION OF THE TEMPERATURE FIELD OF A METAL BARRIER IN COLLISION WITH AN ERODENT PARTICLE

L. I. Urbanovich and E. M. Kramchenkov

UDC 536.24

A numerical model that allows the study of the nonstationary temperature field of a metal barrier in the vicinity of a crater formed due to inelastic impact of a solid spherical particle is considered.

It was found in a study of the mechanism of gas-abrasive erosion of metals and alloys that introduction of a barrier for colliding particles into surface layers can cause a considerable local increase in temperature [1]. This is associated with conversion of a certain portion of the kinetic energy to heat. In [2] it was assumed that local heating up of material layers adjacent to the contact surface leads to softening of the layers and then to erosion failure.

In [1], a quantitative evaluation of local heating up of metals for a limiting case – adiabatic conditions on the assumption that the entire kinetic energy of a particle that it possesses directly before impact converts to heat – is given. At the same time it was noted that the value of the maximum heating up of the surface layers of the material depends greatly on the heat outflow into the depth of the body by heat conduction. However, the authors of [1] did not take this fact into account.

At the same time it is known that in the process of inelastic impact of a particle against a solid surface 1–10% of the kinetic energy is spent on recoil, 1–5% is scattered in the form of elastic waves, and 90% passes to energy of plastic deformation of the barrier (about 75–80% converts to heat, and the remaining portion is conserved in the deformed material in the form of latent energy) [3, 4].

With this fact and the importance of the dependence of the thermophysical properties of the barrier on the temperature in mind, we can formulate the aim of the present paper: the determination of the nonstationary temperature field with account for such factors as the size of the particle, its density, elasticity modulus, and velocity of impact on the one hand and the mechanical and thermophysical properties of the barrier material on the other.

The following assumptions are used:

1) a smooth spherical solid particle of radius r_p and density ρ_p is accelerated by a gas-carrier flow, as is observed in the corresponding experimental setups for studying gas-abrasive erosion [5], and collides with the plane horizontal surface of a metal specimen at a right angle with a velocity w_p; it is implied that Young's modulus E_1 and the Poisson coefficient ν_1 of the particle material are set;

2) the impact is inelastic; heating of the particle is disregarded due to its small mass compared to the mass of the barrier;

3) Young's modulus E_2 and the Poisson coefficient ν_2 of the material of the specimen and its thermophysical properties as a function of the temperature are known;

4) in introduction of a particle into the specimen body a crater is instantaneously formed, the crater has the shape of a spherical segment with a surface area $S = 2\pi r_p h$ through which 75% of the difference in the kinetic energy of the falling and recoiling particle is transferred in the form of heat during the period of plastic indentation τ_p; for this purpose the momentum of the heat flux density as a function of time (at $0 < \tau \leq \tau_p$) is set on the surface of the crater;

5) after a lapse of time τ_p the heated surface transfers heat to the surrounding medium by radiation and convection, and the latter, due to the jet flow of gas along the surface, is forced;

Lipetsk State Technical University, Russia. Translated from Inzhenerno-Fizicheskii Zhurnal, Vol. 72, No. 3, pp. 526-532, May-June, 1999. Original article submitted March 27, 1998.

1062-0125/99/7203-0503$22.00

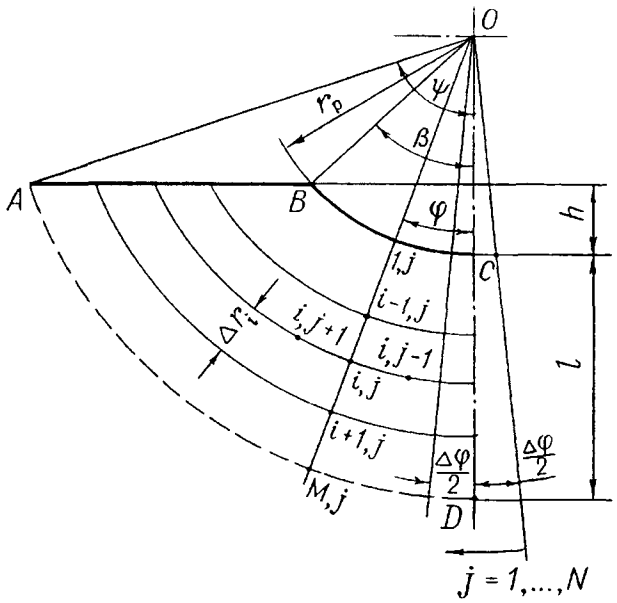

Fig. 1. Schematic illustrating the formulation of the problem.

6) at the initial instant of time the temperature field is uniform;

7) the specimen body is semibounded with respect to heat, i.e., Fo < 1 [6];

8) conforming to the fact that the diameter of the particle is much smaller than the size of the solid body and allowing for the geometric symmetry, we assume that at any instant of time the temperature field is the same for any vertical plane passing through the lower point of a spherical segment (a crater).

Since the temperature field is independent of the longitude, the problem is reduced to the solution of the differential equation of nonstationary heat conduction:

$$\rho(t)\, c(t) \frac{\partial t}{\partial \tau} = \frac{1}{r^2} \frac{\partial}{\partial r} \left(r^2 \lambda(t) \frac{\partial t}{\partial r} \right) + \frac{1}{r^2 \sin \varphi} \frac{\partial}{\partial \varphi} \left(\sin \varphi\, \lambda(t) \frac{\partial t}{\partial \varphi} \right). \tag{1}$$

Here (see Fig. 1) r is the polar radius issuing from the center of the spherical particle at the instant of its contact with the barrier in impact ($r_p \le r \le (r_p + l)$; l is the linear size of the body determined by the condition that Fo $= \lambda\tau/(\rho c l^2) < 1$); and φ is the angle between the polar radius and the vertical axis passing through the center of the sphere, $0 \le \varphi \le \psi$, where

$$\psi = \arccos \left(\frac{r_p - h}{r_p + l} \right). \tag{2}$$

Due to the symmetry of the temperature field with respect to the vertical OD, the calculation is made for half of the cross section, for which a computational grid is constructed as shown in Fig. 1.

The boundary-value conditions include the initial condition

$$t(r, \varphi, 0) = t_{in} \tag{3}$$

and boundary conditions. The first condition is set on the surface of the crater (line BC in Fig. 1):

$$q = \frac{7.8Q}{S\tau_p} \frac{1}{2\pi} \exp \left[- \left(\frac{7.8\tau}{\tau_p} - 3.9 \right)^2 / 2 \right] \quad \text{at} \quad 0 < \tau \le \tau_p, \tag{4}$$

where τ_p is determined by the formula [7]

$$\tau_p = \pi r_p \sqrt{\rho_p / (18 Y_d)}. \tag{5}$$

The depth of the indentation is calculated from the expression [1]

$$h = r_p w_p \sqrt{\left(\frac{2\rho_p}{3H}\right)}, \tag{6}$$

and, as a consequence, the surface area of the crater is

$$S = 2\pi r_p^2 w_p \sqrt{\left(\frac{2\rho_p}{3H}\right)}; \tag{7}$$

the coefficient of restitution $e = w_p'/w_p$ (w_p' is the velocity of the recoiling particle) is found from the equation [7]

$$e = 3.8 \sqrt{\left(\frac{Y_d}{E'}\right)} \left(\frac{2\pi \rho_p w_p^2}{3Y_d}\right)^{-1/8}, \tag{8}$$

where

$$E' = \left(\frac{1-\nu_1^2}{E_1} + \frac{1-\nu_2^2}{E_2}\right)^{-1}. \tag{9}$$

With account for the assumptions made, the quantity of heat Q supplied to the body during the time of impact is expressed as

$$Q = 0.75 \frac{4}{3} \rho_p \frac{\pi r_p^3}{2} w_p^2 (1 - e^2). \tag{10}$$

It is important to note that Q and q (formula (4)) are related by the equation

$$\int_0^{\tau_p} qS\, d\tau = \int_0^1 \frac{7.8Q}{\tau_p} \frac{1}{\sqrt{2\pi}} \exp\left[-\left(\frac{7.8\tau}{\tau_p} - 3.9\right)^2 \Big/ 2\right] d\left(\frac{\tau}{\tau_p}\right) = Q. \tag{11}$$

At $\tau > \tau_p$

$$-\lambda \left(\frac{\partial t}{\partial r}\right)_{r_p} = \alpha_{eff} (t_{r_p} - t_g), \tag{12}$$

where α_{eff} is the effective coefficient of heat transfer, $\alpha_{eff} = \alpha_{con} + \alpha_{rad}$. The coefficient of heat transfer by convection α_{con} is calculated by the formula presented for the given case in [8], and the coefficient of heat transfer by radiation is calculated by the formula

$$\alpha_{rad} = \varepsilon \sigma_0 (T_{r_p}^4 - T_g^4)/(T_{r_p} - T_g). \tag{13}$$

The second boundary condition is set on the plane surface of the specimen (line AB in Fig. 1):

$$-\lambda \left(\frac{\partial t}{\partial r}\right)_{r_p} = \alpha_{eff} (t_{r_p} - t_g) \cos\varphi; \tag{14}$$

the third on the boundary CD at $r_p \le r < (r_p + l)$:

$$\left(\frac{\partial t}{\partial \varphi}\right)_r = 0 \tag{15}$$

and the fourth on the boundary AD:

$$t = t_{\text{in}} . \tag{16}$$

The Kirchhoff substitution [9]

$$\Phi(t) = \frac{1}{\lambda_0} \int_{t_0}^{t} \lambda(t)\, dt , \quad \lambda_0 \frac{\partial \Phi(t)}{\partial t} = \lambda(t) \tag{17}$$

(λ_0 is the coefficient of thermal conductivity at some fixed temperature t_0) and the Goodman substitution [9]

$$h(t) = \int_{t_0}^{t} \rho(t)\, c(t)\, dt , \quad \frac{\partial h(t)}{\partial t} = c'(t) . \tag{18}$$

are used.

Substituting for each material of the barrier a specific function $\lambda(t)$ obtained on the basis of reference data into integral (17) and calculating this integral, it is not difficult to find an expression for the function $\Phi(t)$ and then for the inverse function $t(\Phi)$. Similarly, the functions $h(t)$ and $t(h)$ are found by integral (18).

With account for relations (17) and (18) Eq. (1) is written in the form

$$\frac{\partial h}{\partial \tau} = \lambda_0 \left(\frac{\partial^2 \Phi}{\partial r^2} + \frac{2}{r} \frac{\partial \Phi}{\partial r} + \frac{\cos \varphi}{\sin \varphi} \frac{1}{r^2} \frac{\partial \Phi}{\partial \varphi} + \frac{1}{r^2} \frac{\partial^2 \Phi}{\partial \varphi^2} \right) . \tag{19}$$

To solve Eq. (19) numerically by an explicit method, a computational grid with uniform steps Δr and $\Delta \varphi$ in radius r and angle φ, respectively, is constructed. Setting the number of radii N in the range between r_{p} and $r_{\text{p}} + l$, we can find

$$\Delta \varphi = 2\psi/(2N - 3) . \tag{20}$$

In choosing the step Δr we must satisfy the condition

$$\Delta r \leq (r_{\text{p}} - h)/\cos \left[\left(j_n - \frac{3}{2} \right) \Delta \varphi \right] , \tag{21}$$

where j_n is the number of the radius that is the first to intersect the boundary AB (Fig. 1).

The coordinates of the nodes can easily be expressed in terms of the steps mentioned:

$$r_i = r_{\text{p}} + \Delta r\, (i - 1) , \tag{22}$$

where $i = 1, 2, \ldots, M (M = N - j_n + 2)$,

$$\varphi_j = (j - 1.5)\, \Delta \varphi , \tag{23}$$

where $j = 1, 2, \ldots, N$.

Formula (23) also reflects the fact that additional nodal points lying on the radius $j = 1$ are used, and here the radius is spaced from the vertical OD at an angle equal to $-\Delta \varphi/2$ (see Fig. 1). This approach corresponds to the recommendation given in [10].

The time step $\Delta \tau$ is taken so that its value could simultaneously satisfy the requirements of stability of the computational scheme at the inner nodes and on the boundary ABC [6]:

$$\Delta \tau \leq 0.25/\max \left\{ \frac{\lambda}{c\rho} \left[\frac{1}{\Delta r^2} + 1\, (r_i\, \Delta \varphi)^2 \right] \right\} , \tag{24}$$

$$\Delta\tau \le 0.5/\max\left\{\frac{\lambda}{c\rho}\left[\frac{1}{\Delta r^2}+1\,(r_{j-j_n+2}\,\Delta\varphi)^2\right](2+\mathrm{Bi})\right\}. \tag{25}$$

Then the time of the real process is $\tau = k\Delta\tau$, where $k = 0, 1, 2, \ldots$.

To undertake the calculation of the temperature field one first determines the initial recalculation temperatures and specific enthalpies. For this purpose the temperature t_{in} is substituted into the known functional relations $\Phi = \Phi(t)$ and $h = h(t)$, thus obtaining equal values of Φ_0 and h_0 for all nodes. Having thus formed the arrays $\Phi_{i,j,0}$ and $h_{i,j,0}$ for the instant of time $\tau = 0$, one passes over to the calculation of them at the next instant of time $\tau = \Delta\tau$ $(k = 1)$.

The enthalpy at the inner nodes is found by Eq. (19) reduced to a finite-difference form:

$$h_{i,j,k+1} = h_{i,j,k} + \lambda_0\Delta\tau\left(\frac{\Phi_{i+1,j,k} - 2\Phi_{i,j,k} + \Phi_{i-1,j,k}}{\Delta r^2} + \frac{2}{r_i}\frac{\Phi_{i+1,j,k} - \Phi_{i-1,j,k}}{\Delta r} + \right.$$

$$\left. + \frac{\cos\varphi_j}{\sin\varphi_j}\frac{1}{r_i^2}\frac{\Phi_{i,j+1,k} - \Phi_{i,j-1,k}}{2\Delta\varphi} + \frac{\Phi_{i,j+1,k} - 2\Phi_{i,j,k} + \Phi_{i,j-1,k}}{r_i^2\,\Delta\varphi^2}\right). \tag{26}$$

The set of values $h_{i,j,1}$ at the inner nodes allows one to obtain the arrays $t_{i,j,1}$ and $\Phi_{i,j,1}$ for this region using the functions $t(h)$ and $\Phi(t)$. We present the boundary condition (4) in a finite-difference form:

$$q_k = \frac{7.8Q}{S\tau_p}\frac{1}{\sqrt{2\pi}}\exp\left[-\left(\frac{7.8k\Delta\tau}{\tau_p} - 3.9\right)^2/2\right] \quad \text{for} \quad 0 < k\Delta\tau \le \tau_p. \tag{27}$$

From expression (27) at $k = 1$ we find the value of the heat flux density q_1 for the instant of time $\tau = \Delta\tau$ and then the recalculation temperatures at the outer nodes of the boundary BC:

$$\Phi_{1,j,1} = \Phi_{2,j,1} + q_1\frac{\Delta r}{\lambda_0}. \tag{28}$$

Then, using the functions $t(\Phi)$ and $h(t)$, we come to the arrays $t_{1,j,1}$ and $h_{1,j,1}$ for the outer nodes of the line BC.

To find the arrays $h_{1,j,k}$ and $\Phi_{1,j,k}$ at the nodes at the boundary AB we use the already found array $t_{2,j,1}$ for the nodes lying in the body at a distance Δr from the boundary AB. Addressing ourselves to the boundary condition (12), we present it in finite differences:

$$t_{1,j,k} = \frac{t_{2,j,k} + \alpha_{1,j,k}\dfrac{\Delta r}{\lambda\,(t_{2,j,k})}\,t_g\cos\varphi_j}{1 + \alpha_{1,j,k}\dfrac{\Delta r}{\lambda\,(t_{2,j,k})}\cos\varphi_j}. \tag{29}$$

From formula (29) at $k = 1$ we find the sought values $t_{1,j,1}$ and, consequently, $\Phi_{1,j,1}$, $h_{1,j,1}$ at the boundary AB.

Since the boundary conditions (14), (15) are transformed to the form

$$h_{i,1,k} = h_{i,2,k} \quad \text{and} \quad h_{M,j,k} = h_{in}, \tag{30}$$

respectively, then at $k = 1$ we obtain $h_{i,1,1} = h_{i,2,1}$ at the nodes at the boundary CD and $h_{M,j,1} = h_{in}$ on the line AD.

Clearly, knowledge of the enthalpies at the nodes on the lines CD and AD implies that at these points the temperatures $t_{i,1,1}$ and $\Phi_{i,1,1}$, $t_{M,j,1}$ and $\Phi_{M,j,1}$ are also known.

By this procedure, formation of the arrays of temperatures, recalculation temperatures, and volumetric enthalpies at all nodes of the computational grid for the instant of time $k = 1$ is completed. Then, all arrays with

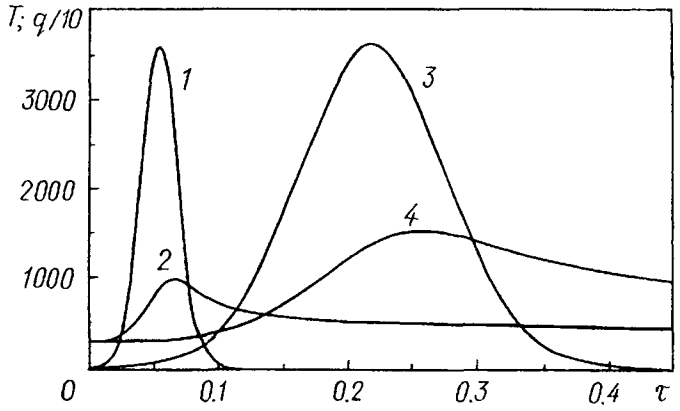

Fig. 2. Time variation of the heat flux density (curves 1, 3) on the surface of a crater and the temperature (curves 2, 4) of a point at a depth of 0.025 μm from the surface of indentation (radius $j = 2$): 1, 2) $d_p = 100$ μm; 3, 4) 400. T, K; $q/10$, MW/m^2; τ, μsec.

the subscript $k + 1$ are reassigned the subscript k, and the calculation proceeds according to the described scheme. On reaching a value $\tau > \tau_p$, the boundary condition (29) is replaced by a modified expression (12):

$$t_{1,j,k} = \frac{t_{2,j,k} + \alpha_{1,j,k} \dfrac{\Delta r}{\lambda\,(t_{2,j,k})}\, t_g}{1 + \alpha_{1,j,k} \dfrac{\Delta r}{\lambda\,(t_{2,j,k})}}, \tag{31}$$

and otherwise the sequence of calculations remains the same as at $\tau < \tau_p$.

Calculations were made for two materials of the barrier with noticeably different thermophysical properties: steels 12Kh18N10T and St. 20 [11]. The particle material is quartz sand.

To evaluate the error of numerical determination of the temperature field, one version (a particle diameter of 100 μm, an impact velocity of 50 m/sec, the barrier material is steel 12Kh18N10T) with a constant time step $\Delta\tau = 5 \cdot 10^{-11}$ sec and twofold differing values of the radius step ($\Delta r_1 = 5 \cdot 10^{-8}$ m and $\Delta r_2 = 2.5 \cdot 10^{-8}$ m; here $\Delta\varphi_1 = 0.0463$ rad and $\Delta\varphi_2 = 0.0484$ rad) was calculated twice. The difference in temperatures at points pertaining to subsurface layers of the crater (where the sharpest change in temperature takes place) turned out to be small. For example, at a depth of 0.1 μm it did not exceed 7 K.

By the curves in Fig. 2 one can judge the change in the heat flux density on the surface of the crater and the surface temperature during the time τ_p of collision of particles of diameter 100 and 400 μm with a barrier made of steel 12Kh18N10T. The curves mentioned are constructed for an impact velocity of 100 m/sec.

We pay attention to the fact that the maxima of the heat flux density in the cases considered (in accordance with relations (5), (6), and (9)) are the same and occur at a time equal to half the impact duration: 0.054 μsec at a particle diameter of 100 μm and 0.219 μsec at a diameter of 400 μm. However, the quantity of heat Q/S transferred during the time of impact through unit surface of the crater to the barrier body amounts to 2.654 kJ/m^2 with the smaller diameter and 10.630 kJ/m^2 with the larger one. This occurs due to the difference in the masses of the particles and the surface areas of the contact. Heating-up of the crater surfaces differs for the same reason: at a diameter of 100 μm the temperature reaches a maximum value equal to 961 K 0.066 μsec from the start of impact, whereas at a diameter of 400 μm the maximum amounts to 1489 K and comes later – in 0.26 μsec. It is characteristic that the temperature maxima are shifted to larger values of time compared to the corresponding extrema of the heat flux density.

Curves 2 and 4 (Fig. 2) indicate that after lapse of the time of impact ($\tau > 0.112$ μsec at a diameter of 100 μm and $\tau > 0.438$ μsec at a diameter of 400 μm) the surface of the indentation is still cooled due to both heat outflow to the depth of the body and radiation and convective transfer to the surrounding medium.

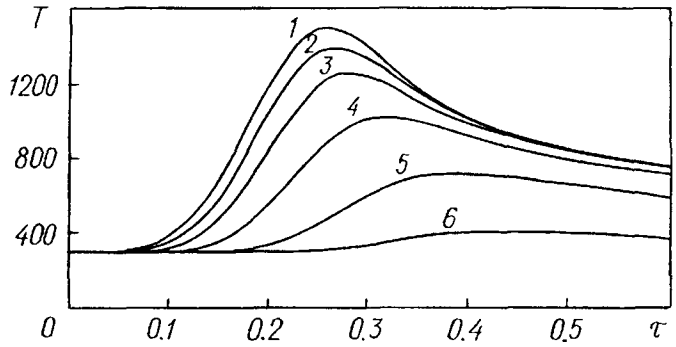

Fig. 3. Time variation of the temperature at points of the barrier body (steel 12Kh18N10T) lying on the same radius $j = 2$ and at different depths from the crater surface: 1) 0.025 μm, 2) 0.1, 3) 0.35, 4) 0.75, 5) 1.45, 6) 2.2.

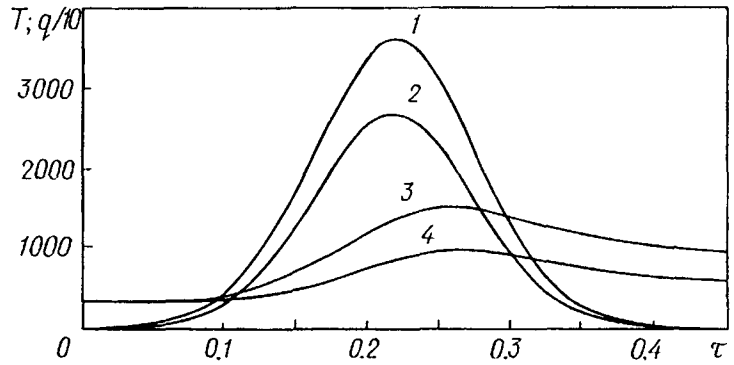

Fig. 4. Time variation of the heat flux density (curves 1, 2) on the crater surface and the temperature (curves 3, 4) of a point at a depth of 0.025 μm from the indentation surface (radius $j = 2$) at a collision velocity of 100 m/sec of a 400-μm-diameter particle: 1, 3) steel 12Kh18N10T; 2, 4) steel St. 20.

From the physical viewpoint it would be natural to expect that not only the size of the particle but also the velocity of impact greatly affect heating-up of the barrier. Calculations confirm this assumption. With an increase in the velocity of a particle having a diameter of 100 μm from 50 to 200 m/sec the quantity of heat supplied to the body increases 17.5-fold with a simultaneous 4-fold growth of the contact surface area, and as a result the maximum temperature of the surface increases from 634 to 1534 K.

The curves constructed in Fig. 3 for six points lying on the same radius ($j = 2$) and at different depths from the crater surface give a representation of the dynamics of heating-up and cooling of different layers of a barrier made of steel 12Kh18N10T. These curves were obtained for an impact velocity of 100 m/sec for a particle with a diameter of 400 μm. It becomes clear from a study of the position of the curves that the substantial heating-up of the surface layers to temperatures of 1500–500 K propagates only to a depth of 2 μm. Moreover, it is obvious that the greater the depth of the layer position the greater the time spent to reach a temperature maximum. In fact, if we consider points at a depth of 0.025 μm (curve 1) and of 2.2 μm (curve 6), then an extremum is reached in 0.2 μsec for the first case and only in 0.4 μsec for the second case (the duration of the impact is 0.438 μsec).

Calculations made for the same conditions of impact but for a specimen made of steel St. 20 whose thermal conductivity differs substantially from that of steel 12Kh18N10T (with an increase in temperature from 293 to 700 K the coefficient of thermal conductivity of steel St. 20 decreases from 51.91 to 31.82 W/(m·K), whereas the coefficient of thermal conductivity of steel 12Kh18N10T increases from 15.1 to 25.9 W/(m·K) [11]) indicate lesser heating-up of all layers. Thus, at a depth of 0.025 μm the largest value of the temperature is 950 K and it is only 330 K at a depth of 2.2 μm, whereas for steel 12Kh18N10T the temperature maxima at these points are, correspondingly, 1489 and 400 K. The reason for the phenomenon observed is not only the higher thermal conductivity of carbon steel but also the smaller amount of heat supplied through the unit surface area of the contact during one and the same time of impact (the area below curve 2 amounts to 74% of the area below curve 1 (see

Fig. 4)). Here one should bear in mind that, with the same amount of heat released in an impact of the same duration, due to the lower hardness of steel St. 20, a crater with a larger contact surface area is formed for this steel than for steel 12Kh18N10T.

Thus, the suggested technique of calculation of the temperature field in the impact zone gives a more authentic picture of local heating-up of a metal compared to [1], due to account for the temperature dependence of thermophysical properties of the material of the barrier in considering heat transfer inside the body and also due to use of boundary conditions that make it possible to allow for radiative and convective heat transfer to the surrounding medium.

NOTATION

ρ, density of the material of the barrier; d_p, diameter of the particle; E_1 and ν_1, Young's modulus and Poisson coefficient of the particle material; E', contact elasticity modulus; Y_d, dynamic yield limit of the material of the target; H, hardness of the barrier; q, heat flux density; t and T, temperature; t_{in}, initial temperature of the target body; t_g, temperature of the gas; c and c', mass and volumetric true specific heat capacity, respectively; h, volumetric specific enthalpy; ε, emissivity of the target surface; σ_0, Stefan–Boltzmann constant; ψ, angle limiting the dimesions of the body of the target for which the temperature field is calculated; $\Delta\varphi$, angle step; M, number of circles of the computational grid; k, number of the time step; Fo, Fourier number; Bi, Biot number. Subscripts: p, particle; d, dynamic; eff, effective; 0, basis temperature; in, initial value; g, gas.

REFERENCES

1. I. M. Hutchings and A. V. Levy, Wear, **131**, 105-121 (1989).
2. P. V. Rao and D. H. Bakley, Translations of ASME, Ser. A [Russian translation], **107**, No. 3, 83-95 (1985).
3. I. M. Hutchings, Wear, **70**, 269-281 (1981).
4. M. A. Bol'shanina and V. E. Panin, Studies in Solid Body Physics [in Russian], Moscow (1957).
5. I. P. Kleis and H. H. Uwemeis, Wear Resistance of Impact Crushers [Russian translation], Moscow (1986).
6. F. Kreit and W. Black, Fundamentals of Heat Transfer [Russian translation (ed. N. A. Anfimov)], Moscow (1983).
7. K. Johnson, Mechanics of Contact Interaction [Russian translation (ed. R. V. Gol'dshtein)], Moscow (1989).
8. D. B. Spalding and D. Taborek, Heat Exchangers – Reference Book [Russian translation (ed. B. S. Petukhov)], Moscow (1987).
9. L. A. Kozdoba, Methods of Solution of Nonlinear Problems of Heat Conduction [in Russian], Moscow (1975).
10. A. V. Luikov, Theory of Heat Conduction [in Russian], Moscow (1967).
11. S. B. Maslenkov and E. A. Maslenkova, High-Temperature Steels and Alloys [in Russian], Moscow (1991).